CRYSTAL
GROWTH
& DESIGN

2005
VOL. 5, NO. 6
2050−2059

Articles

Luminescence Quenching and Energy Transfer in Supramolecular Solids†

Shao-Liang Zheng* and Philip Coppens*

Department of Chemistry, State University of New York at Buffalo, Buffalo, New York 14260-3000

Received June 2, 2005; Revised Manuscript Received July 22, 2005

ABSTRACT: This article summarizes recent progress on the light emission of guest molecules embedded in supramolecular crystals. It covers spectroscopic studies, as well as crystallographic and computational investigations, and focuses on the factors responsible for luminescence quenching in host−guest solids. Examination of energy levels calculated by time-dependent density functional theory and of the experimental host-absorption and guest-emission spectra supports the crucial role of energy level separations in intermolecular energy transfer and the resulting luminescence quenching, thus providing guidelines for the synthesis of long-lifetime luminescent materials.

1. Introduction

One of the prime attractions of the field of crystal engineering is the possibility to tailor-make solids with desirable physical or chemical properties. This is not only the case for bulk properties but also applicable to molecular characteristics, including the spectroscopic behavior of the guest molecules. Supramolecular host matrixes provide a well-defined environment that can be varied by using the methods of crystal engineering and thus offer an attractive possibility to isolate photoactive molecular species in different well-defined states of aggregation and orientation in a dilute yet crystalline environment. Unlike in solutions or rigid glasses, which traditionally have been used for dilution of photoactive species, three-dimensional periodicity is preserved in multicomponent supramolecular solids. In supramolecular solids, the geometric differences in both the ground state and the excited state accompanying the difference in luminescence behavior, and possible distortions of the environment, can be studied by conventional and time-resolved diffraction methods.[1−3] The latter allow identification of excited species and thus interpretation of the photophysical properties at the atomic level. In some cases, the guests may be species not stable otherwise, as is the case for the ligand-unsupported dimer of $(Cu(I)(NH_3)_2)^+$ embedded in an anionic framework.[4]

The topic of energy transfer in solids has drawn considerable attention in the preceding decades. In an excellent review of the triplet state of organic molecules, published in 1965, Lower and El-Sayed drew attention to the difference between deactivation of singlet and triplet states and concluded that the degree of excitation transfer per lifetime of the excited species is greater by a factor of 10^4-10^8 for triplets compared with singlet excited states.[5] Thus, quenching due to intermolecular energy transfer will be much more pronounced in the case of triplet states.

Luminescence quenching also occurs by electron transfer of a weakly bound photoelectron to an electronegative neighboring acceptor molecule, as for example observed in the mixed potassium/methyl viologen salt of the $[Pt_2(pop)_4]^{4-}$ [pop = pyrophosphite, $(H_2P_2O_5)^{2-}$] anion.[6] Such quenching is commonly associated with pronounced color changes which have not been observed in any of the complexes discussed in this article.

Control of luminescence quenching and the corresponding enhancement of the light emission has technological applications in the design of light-emitting diodes and other optical devices.[7,8] With the great advances in structure determination of complex solids, in crystal engineering and in computational chemistry it is opportune to revisit the issue of energy transfer in solids using a combination of the new techniques.

This article describes a number of supramolecular solids with embedded photoactive molecules (Table 1),[9−15] their structures, absorption, and photoluminescence properties as well as computed energy levels, and examines the relationship between the experimental and the theoretical results.

† Dedicated to Prof. J. Michael McBride on the occasion of his 65th birthday.

* To whom correspondence should be addressed. E-mail: coppens@buffalo.edu.

10.1021/cg050247d CCC: $30.25
Published on Web 09/07/2005

Table 1. Low-Temperature Luminescence Lifetimes of Host/Guest Complexes with Photoactive Guests[a]

compound	host framework	lifetime/μs
CMCR-BPY-BZ α,β	2D brick-wall like framework	< ~100 ns[b]
CMCR-2BPE-BZ-S (S = EtOH, $2H_2O$)	2D brick-wall like framework	< ~100 ns[b]
CECR-2BPE-BZ	0D carcerand-like capsule	< ~100 ns[b]
CMCR-2BPEH-BZ-EtOH	1D wavelike chain	< ~100 ns[b]
CMCR-2BIMB-2BZ	1D double-buckled chain	0.58 (77 K)
CMCR-DPP-BZ-EtOH-H_2O	2D wavy layer	0.58 (17 K)
CMCR-3BPY-BZP-$2H_2O$	3D steplike framework	< ~100 ns[b]
CMCR-BPY-BZP-H_2O	2D brick-wall-like framework	< ~100 ns[b]
CMCR-2BPE-BZP	2D brick-wall-like framework	< ~100 ns[b]
CMCR-2BPMH-BZP	3D triple interpenetrating network	< ~100 ns[b]
CMCR-2BPEH-BZP-EtOH	1D wavelike chain	< ~100 ns[b]
CMCR-2BPY-BZP	0D carcerand-like capsule	< ~100 ns[b]
CECR-2BPE-0.5BZP-0.5EtOH	0D carcerand-like capsule	< ~100 ns[b]
CMCR-2BIMB-2BZP	1D double buckled chain	< ~100 ns[b]
CECR-2BIMB-2BZP	1D double buckled chain	< ~100 ns[b]
CMCR-DPP-BZP-2EtOH	2D wavy layer	< ~100 ns[b]
CECR-XT-MeOH	2D layer with deep bowl-shaped cavities	0.22 (17 K)
HECR-2XT-6MeOH	1D wavelike chain	5.56 (17 K)
2DCA-BZP	2D wavelike double layer	3600 (17 K)
CMCR-2BPE-$Ru(Cp)_2$-EtOH	1D wavelike chain	< ~100 ns[b]
2DCA-$Ru(Cp)_2$	2D wavelike double layer	189 (17 K)
2ACA-$Ru(Cp^*)_2$-CCl_3H	2D wavelike double layer	4.4 (17 K)

[a] Abbreviations: ACA = apocholic acid; BIMB = 1,4′-bis(imidazol-1-yl-methyl)benzene; BPE = *trans*-1,4-bis(pyridyl)ethylene; BPMH = bis-(1-pyridin-4-yl-methylidene)-hydrazine; BPEH = bis-(1-pyridin-4-yl-ethylidene)-hydrazine; BPY = 4,4′-bipyridine; BZ = benzil; BZP = benzophenone; CMCR = *C*-methylcalix[4]resorcinarene; CECR = *C*-ethylcalix[4]resorcinarene; DCA = deoxycholic acid; DPP = 1,3-Di-(4-piperidyl)propane; HECR = hexaethylresorcin[6]arene; $Ru(Cp)_2$ = ruthenocene; $Ru(Cp^*)_2$ = decamethylruthenocene; XT = xanthone. [b] Refs 10, 11, and 13. Lifetimes < ~100 ns, which is the detection limit of the equipment in our laboratory.

2. Mechanism of Energy Transfer

The relation between the excited-state lifetime τ and the rate constants for the radiative and nonradiative decay, k_r and k_{nr}, is given by the well-known expression

$$\tau = (k_r + k_{nr})^{-1}$$

Nonradiative decay occurs intramolecularly when excess electronic energy is released into the vibrational modes of the ground state. The detailed theory[16] shows an inverse dependence on the band gap between the excited and the ground states, which has been confirmed by experiment.[17] A major factor affecting photophysical behavior in the solid state is intermolecular energy transfer to the environment, which competes with radiative emission and intramolecular nonradiative deactivation and can lead to full quenching of the emission.

Because of the close packing of molecules and the resulting intermolecular interactions, the short-range mechanism of luminescence quenching is of enhanced importance in solids. Whereas the Coulombic Förster mechanism[18] plays a major role in energy transfer in proteins and in solutions[19] and is the dominant mode of deactivation of excited singlet states at long distances (10−150 Å), it is not a factor in the deactivation of triplet states, as triplet−triplet energy transitions (i.e., $^3D^* + {}^1A \rightarrow {}^1D + {}^3A^*$) of the donor (D) and the acceptor (A) are forbidden.[20] While short range (<10 Å) energy transfer is often attributed to a Dexter exchange mechanism,[21] it has been pointed out that significant orbital-overlap dependent exchange can also be mediated via charge-transfer (CT) configurations.[19,22] The exchange and CT couplings are short range as they depend on overlap of donor and acceptor orbitals, which in the case of a molecule in a supramolecular cavity are the orbitals of the guest and those of the host molecules lining the cavity. Unlike in solutions, in the solid state the molecular orbitals of adjacent molecules have a well-defined spatial relationship so that the orbital-overlap dependent $^3D^* + {}^1A \rightarrow {}^1D + {}^3A^*$ exchange mechanism will be enhanced.

Scheme 1. Schematic of Guest−Host Singlet and Triplet Energy Transfer Mechanisms in Crystalline Supramolecular Inclusion Complexes[a]

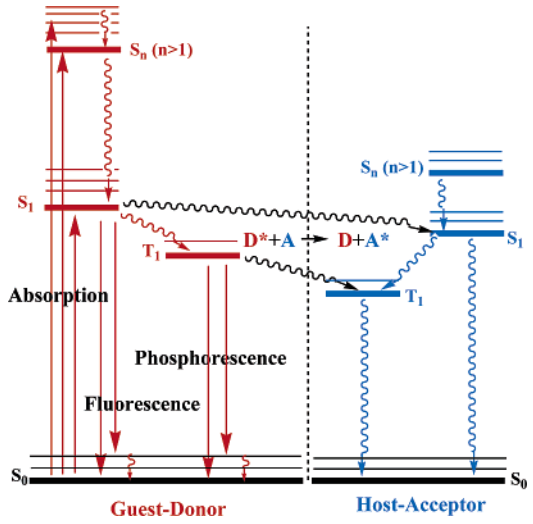

[a] Straight arrows: radiative processes; wavy arrows: nonradiative processes.

3. Comparison of Guest Emission and Host Absorption Spectra

Both long- and short-range energy transfer depend on the energy level spacings of the donor which is deactivated and the acceptor (Scheme 1).[23] Although in many discussions of energy transfer such information is derived from the presence or absence of overlap between the guest emission and the host absorption spectra, this criterion may be misleading. In many cases, the longest-wavelength absorption maxima in the UV spectra correspond not to the S_0-S_1 transition but to transitions S_0-S_n with $n > 1$, as the oscillator strength of the S_0-S_1 transition may be very small.[24,25]

Scheme 2. Structure of (a) BZ, (b) BZP, (c) XT, (d) CMCR, CECR, (e) HECR, (f) BPE, (g) BPEH, (h) BPY, (i) BIMB, (j) DPP (k) DCA, (l) ACA, (m) THPE[a]

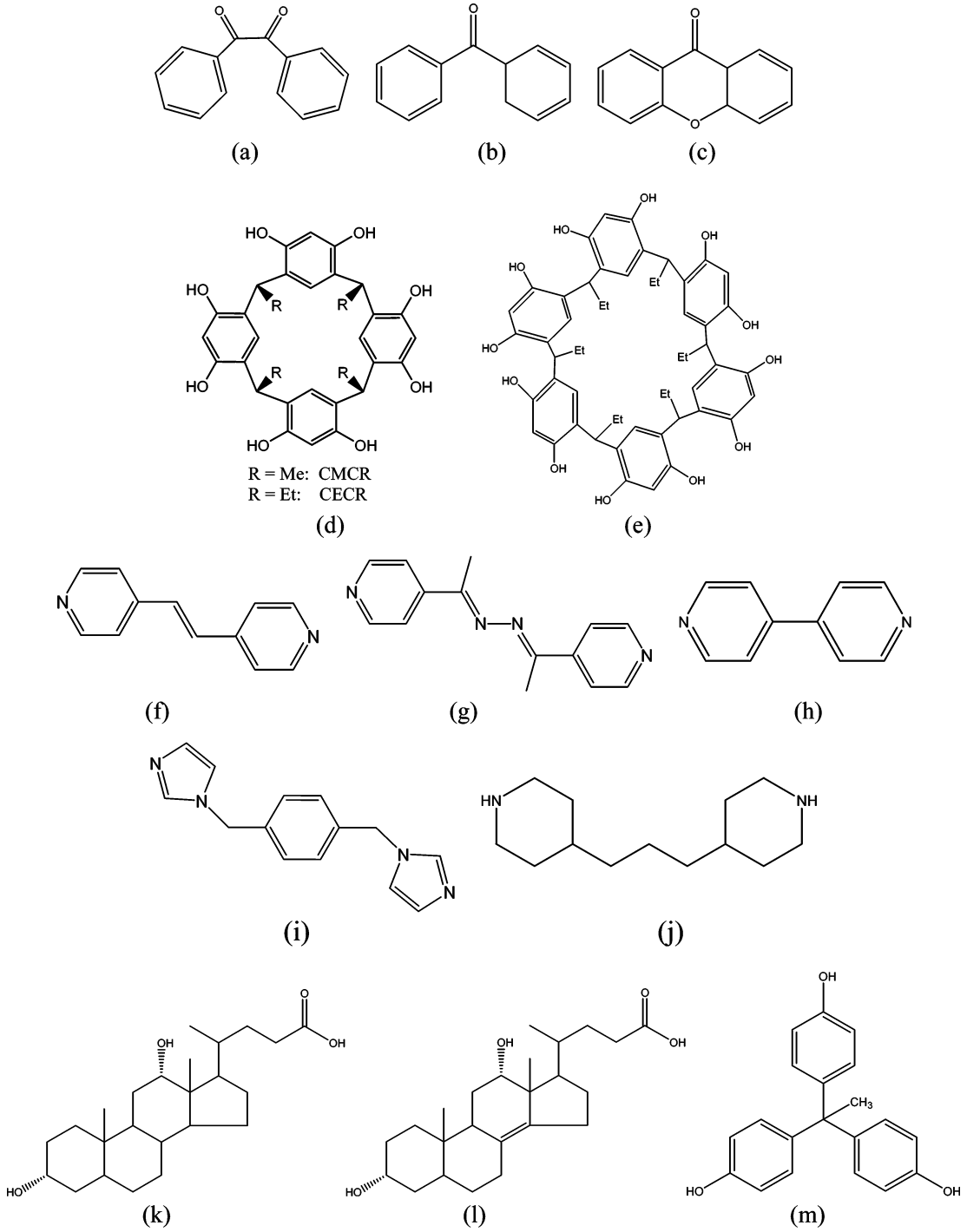

[a] Abbreviations: ACA = apocholic acid; BIMB = 1,4′-bis(imidazol-1-yl-methyl)benzene; BPE = *trans*-1,4-bis(pyridyl)ethylene; BPMH = bis-(1-pyridin-4-yl-methylidene)-hydrazine; BPEH = bis-(1-pyridin-4-yl-ethylidene)-hydrazine; BPY = 4,4′-bipyridine; BZ = benzil; BZP = benzophenone; CMCR = *C*-methylcalix[4]resorcinarene; CECR = *C*-ethylcalix[4]resorcinarene; DCA = deoxycholic acid; DPP = 1,3-di-(4-piperidyl)propane; HECR = hexaethylresorcin[6]arene; $Ru(Cp)_2$ = ruthenocene; $Ru(Cp^*)_2$ = decamethylruthenocene; XT = xanthone.

Such transitions are allowed in energy transfer mediated by the short-range energy transfer mechanism.[20] Thus, although overlap of the emission and absorption bands is conclusive, its absence cannot be used as evidence that energy transfer does not take place.

It may also be noted that the emission spectra can be very sensitive to the degree of aggregation.[26] This is particularly true for excimers or exciplexes, which show pronounced red-shifts compared with the monomeric species.[25,27] Thus, comparison with the emission spectra of the isolated guest component is not always appropriate.

4. MO Calculations of Excited State Energy Levels

The development of time-dependent density functional theory (TDDFT) has opened the possibility of

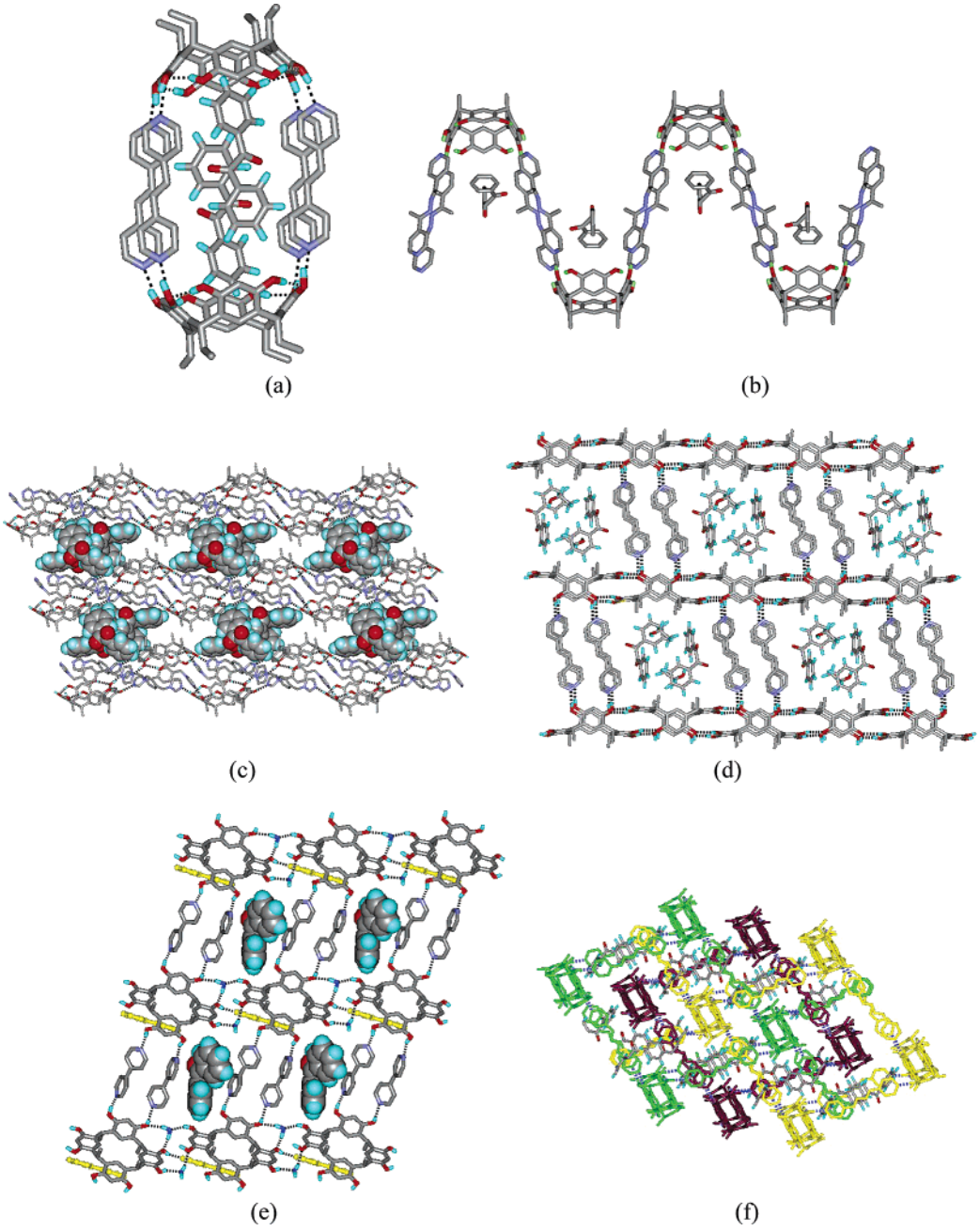

Figure 1. Supramolecular solids incorporating photoactive molecules: (a) 0D carcerand-like capsule in CECR-2BPE-BZ,[10](b) 1D wavelike chain in CMCR-2BPEH-BZ-EtOH (The BZ molecule is disordered, only one orientation is shown),[13] (c) 1D double-buckled chain in CMCR-2BIMB-2BZ,[11] (d) 2D brick-wall like framework in CMCR-2BPE-BZ-EtOH,[10] (e) 3D stepped framework in CMCR-3BPY-BZP-2H_2O,[13] and (f) 3D triply interpenetrating network in CMCR-2BPMH-BZP.[13]

calculation of the wave functions and energies of excited singlet and triplet states, and thereby obtain ES−GS energy gaps to identify spectroscopically observed transitions, and corresponding oscillator strengths. In the current work, TDDFT as implemented in Gaussian03[28] has been used.

It is necessary to keep in mind that the energy levels calculated for isolated molecules will be affected by incorporation of the species as guest into the host framework. Molecular interactions in the solid state, such as hydrogen bonding and $\pi-\pi$ stacking, can reduce the ES−GS separations, as is evident in band structure formation in organic solids[29] and from other observations.[30]

5. Selected Examples of Guests in Organic Host Environments

5.1 Components of the Host Lattices Examined. The resorcinarenes, such as CMCR, CECR, HECR (CMCR = *C*-methylcalix[4]resorcinarene, CECR = *C*-ethylcalix[4]resorcinarene, HECR = hexaethylresorcin-[6]arene, Scheme 2d,e), are versatile building blocks that can generate a remarkable variety of different frameworks with spacers such as 4,4′-bipyridine (BPY), *trans*-1,4-bis(pyridyl)ethylene (BPE), bis-(1-pyridin-4-yl-ethylidene)-hydrazine (BPEH), 1,4′-bis(imidazol-1-yl-methyl)benzene (BIMB), and 1,3-di-(4-piperidyl)propane (DPP, Scheme 2f−j). As shown in Figure 1, they include

Table 2. Calculated Excited State Energy Separations and Oscillator Strengths of (a) Guest Molecules, (b) Framework Molecules, and (c) Linker Molecules

(a) Guest Molecules

	BZ	BZP	monomer XT	dimer XT
energy separation	*E*/eV (*f*)	*E*/eV (*f*)	*E*/eV (*f*)	*E*/eV (*f*)
S_0-T_1	2.281 (0.000)	2.939 (0.000)	3.148 (0.000)	2.887 (0.000)
S_0-S_1	2.785 (0.000)	3.564 (0.001)	3.710 (0.000)	3.622 (0.000)
S_0-S_2	3.761 (0.001)	4.587 (0.012)	3.988 (0.061)	3.623 (0.000)
S_0-S_3	4.183 (0.028)	4.652 (0.034)	4.730 (0.054)	3.900 (0.000)
S_0-S_4	4.191 (0.001)	4.759 (0.260)	5.059 (0.021)	3.948 (0.002)
S_0-S_5	4.276 (0.218)	4.969 (0.037)	5.249 (0.308)	3.993 (0.094)

(b) Framework Molecules

	CMCR	CECR	HECR	DCA	ACA
energy separation	*E*/eV (*f*)	*E*/eV (*f*)	*E*/eV (*f*)	*E*/eV (*f*)	*E*/eV (*f*)
S_0-T_1	3.531 (0.000)	3.532 (0.000)	3.575 (0.000)	5.065 (0.000)	3.762 (0.000)
S_0-S_1	3.888 (0.000)	4.083 (0.000)	4.262 (0.000)	5.640 (0.001)	5.747 (0.001)
S_0-S_2	4.270 (0.008)	4.254 (0.040)	4.270 (0.035)	7.001 (0.004)	5.7941 (0.000)
S_0-S_3	4.434 (0.036)	4.297 (0.037)	4.397 (0.000)	7.083 (0.000)	6.4489 (0.469)

(c) Linker Molecules

	BPE	BPEH	BPY	BIMB	DPP
energy separation	*E*/eV (*f*)	*E*/eV (*f*)	*E*/eV (*f*)	*E*/eV (*f*)	*E*/eV (*f*)
S_0-T_1	2.383 (0.000)	2.665 (0.000)	3.461 (0.000)	3.674 (0.000)	6.465 (0.000)
S_0-S_1	4.005 (0.001)	3.481 (0.000)	4.405 (0.005)	4.745 (0.000)	6.863 (0.006)
S_0-S_2	4.016 (0.003)	3.934 (0.362)	4.447 (0.002)	4.750 (0.002)	6.994 (0.018)
S_0-S_3	4.160 (0.899)	4.055 (0.002)	4.985 (0.005)	4.934 (0.003)	7.400 (0.026)
S_0-S_4	4.499 (0.045)	4.073 (0.028)	5.030 (0.037)	4.925 (0.002)	7.657 (0.007)
S_0-S_5	4.502 (0.000)	4.479 (0.321)	5.153 (0.000)	5.287 (0.000)	7.672 (0.007)
S_0-S_6	4.499 (0.000)	4.516 (0.013)	5.162 (0.000)	5.656 (0.156)	7.806 (0.027)

the 0D carcerand-like capsule, 1D wavelike chain, 1D double-buckled chain, 2D brick-wall-like framework, 3D steplike framework, and 3D triple interpenetrating network. Deoxycholic acid (DCA) and its analogue, apocholic acid (ACA, Scheme 2k,l) can incorporate a large variety of guests and, because the absence of aromatic rings in these molecules, provide an excellent comparison with less saturated framework components. THPE (THPE = trihydroxyphenylethylene, Scheme 2m) forms anionic hydrogen-bonded frameworks when combined with cations, which allow incorporation of metalloorganic cations.

5.2 Organic Guest Molecules. 5.2.1 Benzil in Resorcinarene-Linker Inclusion Complexes. Aromatic ketones, such as benzil (BZ),[31] benzophenone (BZP),[32] and xanthone (XT, Scheme 2a–c),[33,34] are of particular interest as they have excited n–π^* and $\pi-\pi^*$ triplet states with lifetimes as high as milliseconds at low temperature in the solid state or rigid media.

Emission measurements show that in a series of supramolecular solids based on resorcinarene and bipyridyl-type conjugated linker molecules, the intense phosphorescence of BZ is completely quenched, even at 17 K.[11] The quenching is reduced when the nonconjugated linker molecule BIMB,[11] or the fully saturated DPP[12] linker molecule are used to connect the CMCR molecules, although even in that case the lifetime (Table 1) is very much shorter than the corresponding lifetime of BZ in its neat crystals (1.5 ms at 77 K[11] and 4.0 ms at 17 K.[12]

To explain the considerable reduction in lifetime, we examine both the experimental spectroscopic data and the theoretical energy levels of the components in supramolecular solids.[12] The energy levels from TDDFT calculations (Table 2) indicate that except for the fully saturated linker DPP, the ES–GS separations of isolated CMCR and linker molecules are only slightly larger than those of the BZ guest. With some energy-gap lowering due to intermolecular interactions between the CMCR and the linker molecules, the energy gaps in the host framework will be very similar to those of the BZ guest, allowing significant energy transfer and corresponding luminescence quenching. On the other hand, neat BZ crystals emit at ca. 525 nm upon 337 nm excitation at room temperature, and the absorption bands of a powder prepared from clear CMCR crystals[35] occur in the 210–400 nm region, whereas the absorption of the fully saturated linker, DPP ligand, lies significantly further into the ultraviolet (210–280 nm) than the other bipyridyl-type conjugated or nonconjugated linker molecules (Figure 2). Notwithstanding the lack

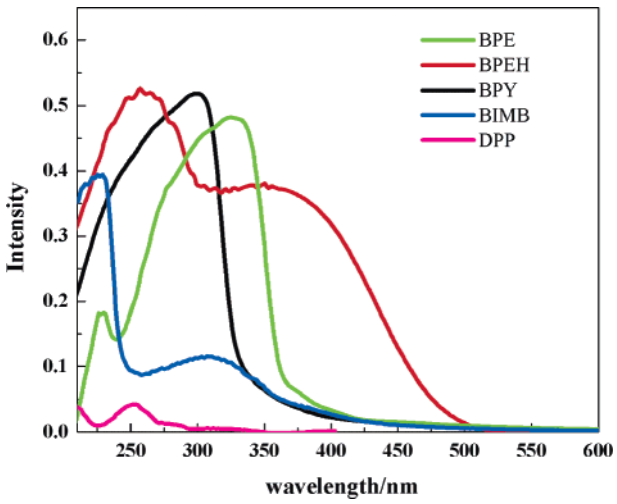

Figure 2. The solid UV spectra of various linkers.

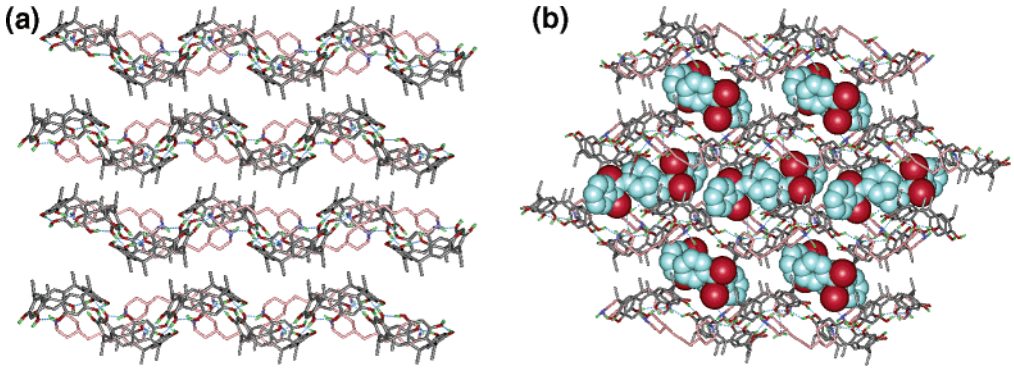

Figure 3. Three-dimensional supramolecular architecture of (a) the benzil-free complex CMCR-DPP-3EtOH and (b) corresponding host−guest system CMCR-DPP-BZ-EtOH-H_2O.

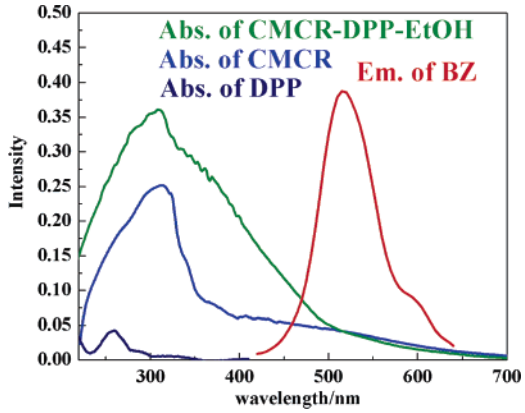

Figure 4. The emission spectrum of the BZ guest molecules and the absorption spectra of CMCR, DPP, and the benzil-free complex CMCR-DPP-3EtOH.

of overlap of the absorption and emission spectra, the 17 K lifetime of BZ in CMCR-DPP-BZ-EtOH-H_2O is only 0.58 μs (Table 1), orders of magnitude below the 4 ms observed for neat BZ at the same temperature.

To examine the spectroscopic properties of an assembly of framework-only components, a benzil-free analogue of CMCR-DPP-BZ-EtOH-H_2O, CMCR-DPP-3EtOH (Figure 3), was prepared. Compared with the isolated components of the host framework, the absorption bands of the framework-like analogue have shoulders extending as far as 475 nm, confirming the effect of the solid assembly on spectroscopic properties, and leading to overlap of the framework-absorption with the BZ emission spectrum (Figure 4). Equally important, the energy level analysis indicates that the longest-wavelength absorption maxima of the CMCR-DPP assembly correspond to S_0-S_n transitions with $n \geq 1$. Thus, the observed emission quenching of BZ in CMCR-DPP and in other CMCR-unsaturated-linker framework solids can be readily understood.

5.2.2 Benzophenone in Resorcinarene-Linker Inclusion Complexes. In parallel studies, similar emission quenching has been observed in a series of supramolecular solids containing BZP. Taking into account that the corresponding ES−GS separations of the BZP molecule are larger than those of BZ (Table 2), which enhances the energy transfer by decreasing the difference in energy level spacings between the guest and the host framework, the emission quenching of BZP can similarly be attributed to the energy transfer from the guest to the host framework in supramolecular solid.

5.2.3 Xanthone in Resorcinarene-Based Supramolecular Host/Guest Solids. The analysis of luminescence behavior is simplified when inclusion compounds without linker molecules can be synthesized. Two such resorcinarene-based complexes incorporating XT (Scheme

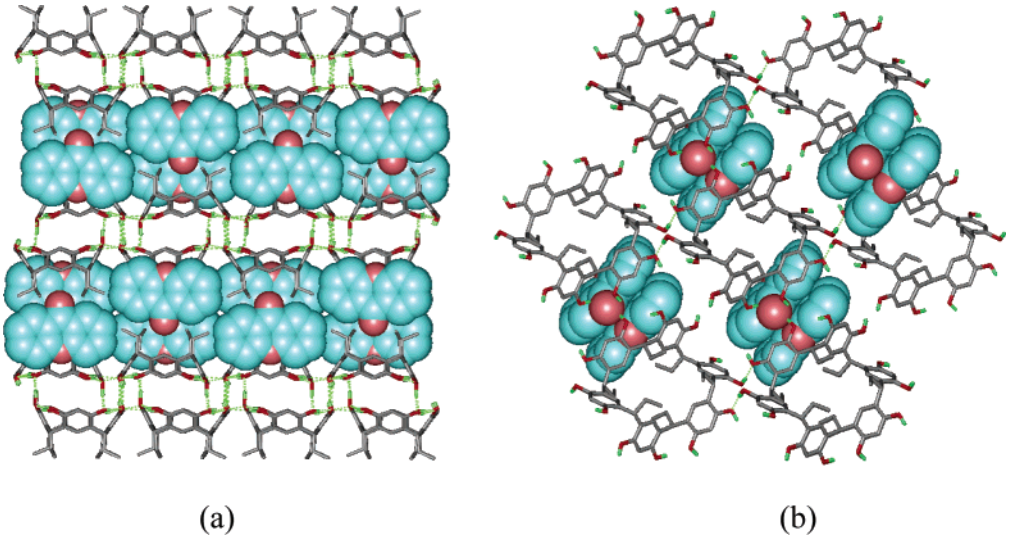

Figure 5. Three-dimensional supramolecular architecture of (a) CECR-XT-MeOH, containing monomer XT, and (b) HECR-2XT-6MeOH, containing dimeric XT.

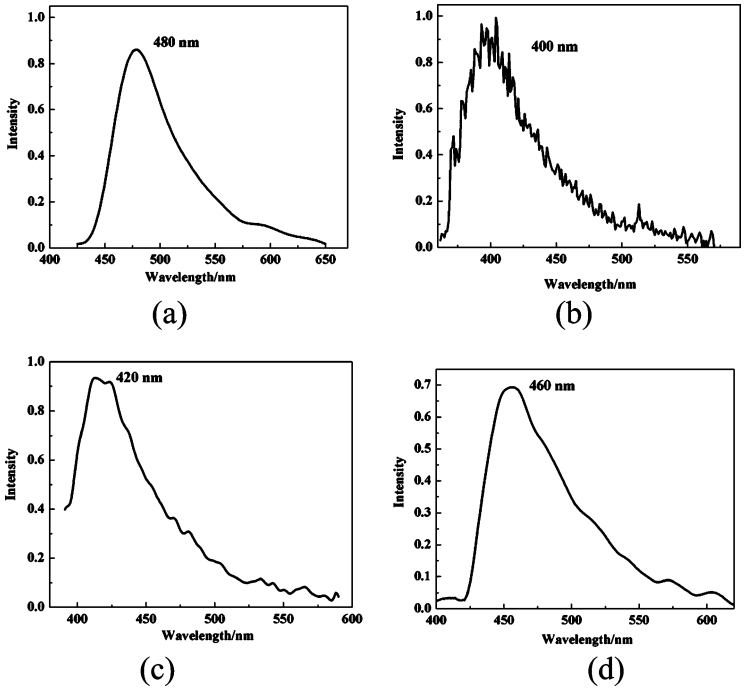

Figure 6. The emission spectra of XT (a) in the solid state at 17 K, (b) in hexane solution at room temperature, (c) in CECR-XT-MeOH, and (d) in HECR-2XT-6MeOH at 17 K.

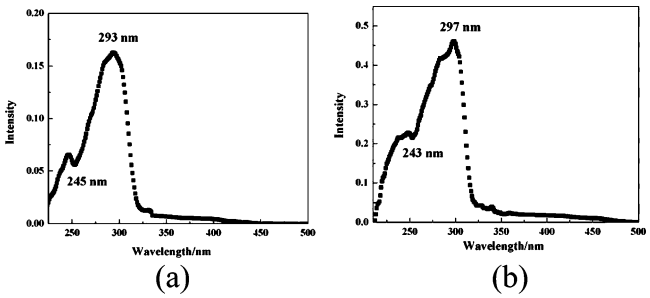

Figure 7. The UV−vis spectra in the solid state for (a) CECR and (b) HECR.

1c), CECR-XT-MeOH, and HECR-2XT-6MeOH were prepared.[9] The XT molecule occurs as monomer trapped in a 2D layer with deep bowl-shaped cavities and as a dimer located in the channel between 1D wavelike chains (Figure 5), respectively, resulting in a 40 nm shift of the longest wavelength absorption band (Figure 6).

Similar to CMCR, the absorption bands of a powder prepared from clear CECR or HECR crystals[35] occur in the 210−400 nm region (Figure 7), while XT in its neat crystals emits at ca. 480 nm (Figure 6a), suggesting that no significant overlap between the emission spectrum of guest and the absorption spectrum of host framework exists. However, the room-temperature emission spectrum of XT dissolved in hexane is blue-shifted to ca. 400 nm (Figure 6b), demonstrating the effect of molecular interactions. Furthermore, the longest-wavelength absorption maxima in the UV spectra of CECR, and HECR correspond to S_0-S_n transitions with $n > 1$ (Table 2) and are thus not characteristic for the energy gaps that can play a role in the short-range energy transfer. The TDDFT calculations on the isolated molecules indicate that the S_0-S_1 gaps of CECR or HECR are only slightly larger than those of the XT guest. Thus, taking into account the effect of molecule−molecule interactions, the energy gap of the host framework is likely to be

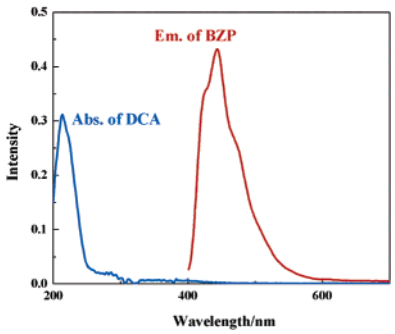

Figure 8. The emission spectrum of the BZP guest molecules and the absorption of the DCA host.

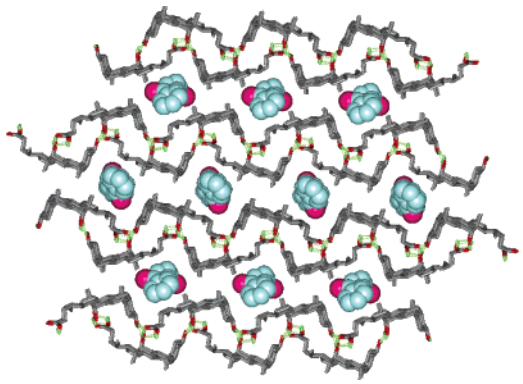

Figure 9. Three-dimensional supramolecular architecture of 2DCA-BZP.

similar to that of XT guest, thus allowing significant energy transfer and quenching of the luminescence. The effect is pronounced, the 17 K lifetime of the emission in the CECR-XT-MeOH complex is only 0.22 μs, compared with 887 μs for neat XT.[9]

For dimeric XT in HECR-2XT-6MeOH the emission is significantly red-shifted, in agreement with calculated

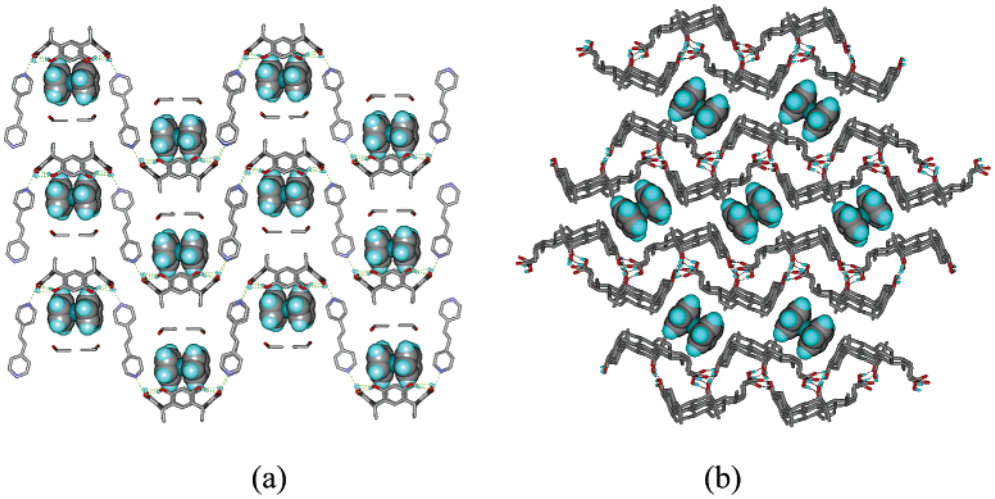

Figure 10. Three-dimensional supramolecular architecture of (a) CMCR-2BPE-Ru(Cp)$_2$-EtOH and (b) 2DCA-Ru(Cp)$_2$.

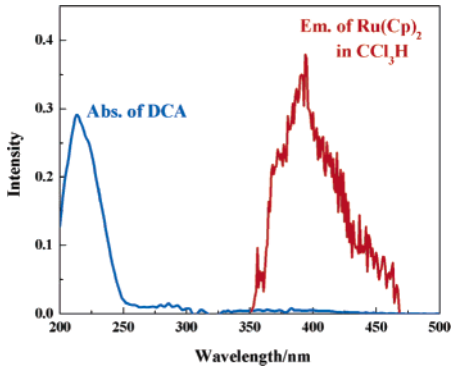

Figure 11. The emission spectrum of Ru(Cp)$_2$ in chloroform at room temperature, and the absorption of the DCA host.

ES−GS separations for the dimer. The observed reduction of luminescence quenching ($\tau_{17K} = 5.56\ \mu s$) for the dimer relative to the monomer may thus be attributed to the reduced ES(triplet)−GS(singlet) energy gap of the XT donor, which becomes smaller than the corresponding gap of the host acceptor molecules. In a time-resolved diffraction study, to be reported elsewhere, we find a considerable contraction of the interplanar distance upon formation of the triplet XT excimer in HECR-2XT-6MeOH.[36]

5.2.4 Benzophenone in Deoxycholic Acid. For DCA, the calculated ES−GS separations are much larger than for BZP (Table 2). In agreement with this, the neat BZP crystals emit at ca. 445 nm upon 337 nm excitation at room temperature, while the absorption bands of DCA are in the 214−260 nm region (Figure 8), thus suggesting that luminescent supramolecular materials can be synthesized using these components. This is indeed the case. In 2DCA-BZP, the BZP molecules are located in the channels between 2D wavelike DCA hydrogen-bonded double layers (Figure 9). As anticipated, upon 366 nm excitation at 17 K the compound exhibits intense photoluminescence with an emission maximum at ca. 450 nm. At this temperature, the lifetime is 3.6 ms, which exceeds the 2.2 ms lifetime for neat BZP.

5.3 Organometallic Guests. So far, we have treated only organic luminescent guest molecules and in particular aromatic ketones. The arguments presented are equally valid for included organometalic guests. Although fewer examples have been described in the literature, many organometallic complexes can be readily included in host frameworks. An example is the complex CMCR-2BPE-Ru(Cp)$_2$-EtOH (Figure 10a) [Ru(Cp)$_2$ = ruthenocene].[14b] The emission properties of the Ru(Cp)$_2$ guest molecule in its neat crystals have been the subject of a number of studies.[37,38] In CMCR-2BPE-Ru(Cp)$_2$-EtOH the emission of Ru(Cp)$_2$ is fully quenched even at low temperature (Table 1). On the other hand Ru-

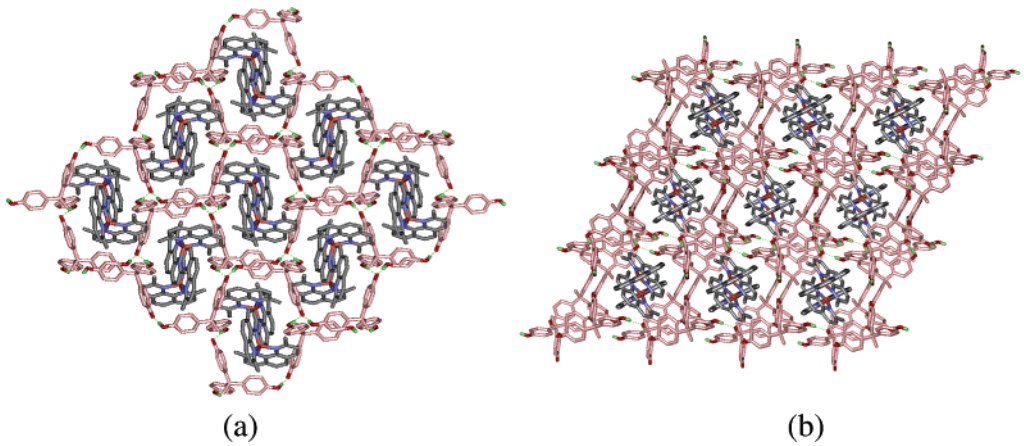

Figure 12. Three-dimensional supramolecular architecture of (a) Cu(dmp)$_2$-(THPE)$^-$ and (b) Cu(dmp)$_2$-(2THPE)$^-$ -H$_2$O.

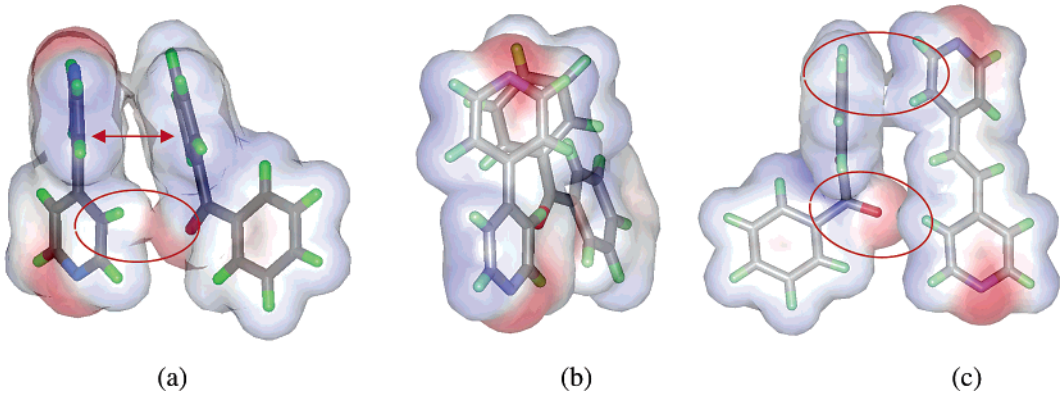

Figure 13. (a, b) Intermolecular interactions between BZP and BPY in CMCR-3BPY-BZP-2H_2O[13] [interplanar distance of 3.45 Å, (C)-H···O distance of 2.55 Å], and (c) the intermolecular interactions between BZ and BPE in CMCR-BPE-BZ-EtOH[10] [perpendicular distance of 3.66 Å from C(H) to benzene ring, (C)-H···O distance of 2.70 Å]. Surfaces shown are defined by the atomic van der Waals radii.

$(Cp)_2$ phosphoresces with a 17 K lifetime of 189 μs in 2DCA-$Ru(Cp)_2$,[15] in which it occurs as an isolated monomer (Figure 10b). In a chloroform solution at room temperature it emits at ca. 395 nm upon 280 nm excitation.[15] There is no significant overlap of this emission with the absorption of the host DCA molecules (Figure 11). As observed for the BZP emission in 2DCA-BZP, the emission lifetime of the DCA inclusion complex exceeds that of neat $Ru(Cp)_2$ (187 vs 127 μs) at 17 K, thus confirming the importance of the large energy-level spacings of the saturated DCA molecule.

The lifetime of penta-methyl substituted complex, $Ru(Cp^*)_2$ [$Ru(Cp^*)_2$ = decamethylruthenocene] is considerable larger (527 μs) at 17 K, but the emission is strongly quenched in a host framework consisting of the partially unsaturated ACA molecule: in 2ACA-$Ru(Cp^*)_2$-CCl_3H[15] the lifetime of $Ru(Cp^*)_2$ is only 4.4 μs at 17 K (Table 1), in agreement with the smaller ES−GS energy gap of ACA compared with DCA (Table 2).

The emission lifetimes of the $Cu(dmp)_2^+$ (dmp = 2,9-dimethyl-[1,10]phenanthroline) ion show considerable variation depending on the counterion in a series of neat crystals. In our study of 11 salts of $Cu(dmp)_2^+$ lifetimes ranged from (RT/17 K) 180/300 ns for the calixerate salt to 950/2400 ns for the *p*-tosylate.[39] $Cu(dmp)_2^+$ can be trapped in an extended framework using THPE,[40] to give $Cu(dmp)_2$-$(THPE)^-$ and $Cu(dmp)_2$-$(2THPE)^-$ -H_2O (Figure 12). It is interesting that no significant shortening of the lifetime relative to that of the other salts occurs in this anionic framework, the $Cu(dmp)_2^+$ lifetimes being (RT/17 K) 310/700 ns and 670/1260 ns for $Cu(dmp)_2$-$(THPE)^-$ and $Cu(dmp)_2$-$(2THPE)^-$ -H_2O, respectively. Of course, no comparison with the lifetime of an "emitter-only" crystal is possible in this case.

6. The Effect of Molecular Orientation

The theory of triplet state deactivation by short-range energy transfer requires overlap of the donor and acceptor orbitals involved. Such overlap is indeed evident in some of the supramolecular solids based on resorcinarene and bipyridyl-type conjugated linker molecules (see for example Figure 13). On the other hand, the absence of overlap between the π-systems in CECR-XT-MeOH is striking (Figure 14), given the fact that

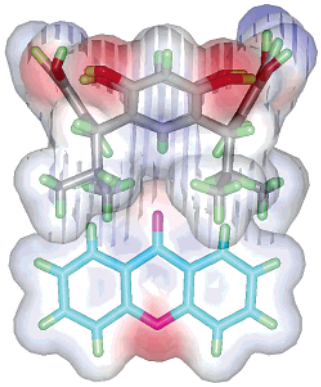

Figure 14. Absence guest−donor/host−acceptor orbital interactions between XT and CECR in CECR-XT-MeOH. Surfaces shown are defined by the atomic van der Waals radii.

the XT luminescence is strongly quenched, suggesting that the overlap criterion is less stringent.

7. Conclusions

It is evident that the lowest ground state-excited state energy level gap cannot be readily obtained from the absorption spectra because due to low oscillator strength the longest wavelength band observed may not correspond to the S_0−S_1 transition. However, combined examination of experimental host-absorption and guest-emission spectra and TDDFT-calculated energy levels provides a basis for interpretation of the experimental results. Our results confirm the crucial role of the energy level separations in the energy transfer process. They must be taken into account in the design of supramolecular host−guest solids with long-lifetime excited states. When this is done, strongly luminescent supramolecular systems can be obtained via rational synthetic strategies. The effect of molecular orientation is less evident in the solids surveyed here and requires further attention.

Acknowledgment. We would like to thank Dr. Irina Novozhilova for assistance with the calculations and Dr. Andrey Yu. Kovalesky, Dr. Oksana Gerlits, and Dr. Bao-Qing Ma for helpful discussions at the beginning of this work. We thank Dr. Qing-Dong Zheng for recording the solution spectra presented in this study. Support of this

work by the National Science Foundation (CHE0236317) and the Petroleum Research Fund of the American Chemical Society (PRF32638AC3) is gratefully acknowledged.

References

(1) Coppens, P.; Ma, B.-Q.; Gerlits, O.; Zhang Y.; Kulshrestha, P. *CrystEngComm* **2002**, *4*, 302−309.

(2) (a) Coppens, P.; Novozhilova, I. V. *Faraday Discuss.* **2003**, *122,* 1−11. (b) Coppens, P. *Chem. Commun*. **2003**, 1317−1320. (c) Coppens, P.; Vorontsov, I. I.; Graber, T.; Gembicky, M.; Kovalevsky, A. Yu. *Acta Crystallogr. A* **2005**, *61*, 162−172.

(3) (a) Coppens, P.; Vorontsov, I. I.; Graber, T.; Kovalevsky, A. Yu.; Chen, Y.-S.; Wu, G.; Gembicky, M.; Novozhilova, I. V. *J. Am. Chem. Soc.* **2004**, *126*, 5980−5981. (b) Coppens, P.; Gerlits, O.; Vorontsov, I. I.; Kovalevsky, A. Yu.; Chen, Y.-S.; Graber, T.; Novozhilova, I. V. *Chem. Commun*. **2004**, 2144−2145. (c) Vorontsov, I. I.; Kovalevsky, A. Yu.; Chen, Y.-S.; Graber, T.; Novozhilova, I. V.; Omary, M. A.; Coppens, P. *Phys. Rev. Lett.* **2005**, *94*, 193003-1−193003-4.

(4) Zheng, S.-L.; Messerschmidt, M.; Coppens, P. *Angew. Chem., Int. Ed.* **2005**, *44*, 4614−4617.

(5) Lower, S. K.; El-Sayed, M. A. *Chem. Rev.* **1966**, *66*, 199−241.

(6) (a) Gerlits, O.; Kovalesky, A. Yu.; Coppens, P., unpublished results. (b) Gerlits, O. Ph.D. Thesis, State University of New York at Buffalo, 2005.

(7) Sudhakar, M.; Djurovich, P. I.; Hogen-Esch, T. E.; Thompson, M. E. *J. Am. Chem. Soc.* **2003**, *125*, 7796−7797.

(8) Tanaka, I.; Tabata, Y.; Tokito, S. *Chem. Phys. Lett.* **2004**, *400*, 86−89.

(9) Zheng, S.-L.; Coppens, P. *Chem. Eur. J.* **2005**, *11*, 3583−3590.

(10) Ma, B.-Q.; Zhang, Y.; Coppens, P. *J. Org. Chem.* **2003**, *68*, 9467−9472.

(11) Ma, B.-Q.; Vieira Ferreira, L. F.; Coppens, P. *Org. Lett.* **2004**, *6*, 1087−1090.

(12) Zheng, S.-L.; Coppens, P. *CrystEngComm* **2005**, *7*, 289−293.

(13) (a) Ma, B.-Q.; Coppens, P. *Cryst. Growth Des.* **2004**, *4*, 1377−1385. (b) Zheng, S.-L.; Coppens, P., unpublished results: CMCR-DPP−BZP-2EtOH: $P2_1/n$, a (Å) = 15.2774, b (Å) = 24.9377, c (Å) = 15.7096, β (°) = 91.649, V (Å^3) = 5982.6.

(14) (a) Zhang, Y. G.; Kim, C. D.; Coppens, P. *Chem. Commun*. **2000**, 2299−2230. (b) Ma, B.-Q.; Coppens, P. *Chem. Commun*. **2003**, 504−505.

(15) Zheng S.-L.; Coppens, P. unpublished results: 2DCA-BZP: $P2_12_12_1$; a (Å) = 25.5510, b (Å) = 13.6515, c (Å) = 7.1526, V (Å^3) = 2494.8; 2DCA-Ru(Cp)$_2$: $P2_12_12_1$: a (Å) = 27.0146, b (Å) = 13.6922, c (Å) = 13.9442, V (Å^3) = 5157.8; 2ACA-Ru(Cp*)$_2$−CCl_3H: $P2_1$: a (Å) = 28.6905, b (Å) = 30.4820, c (Å) = 7.5012, β (°) = 96.0269, V (Å^3) = 6523.9.

(16) Freed, K. F.; Jortner, J. *J. Chem. Phys.* **1970**, *52*, 6272−6291.

(17) See for example: Scaltrito, D. V.; Thompson, D. W.; O'Callaghan, J. A.; Meyer, G. J. *Coord. Chem. Rev.* **2000**, *208*, 243−266.

(18) Förster, Th. Delocalized Excitation and Excitation Transfer. In *Modern Quantum Chemistry*; Sinanoglu, O., Ed.; Academic Press: New York, 1965; pp 93−137, Vol. 3.

(19) Andrews, D. L.; Demidov, A. A. *Resonance Energy Transfer*; John Wiley & Sons: Chichester, 1999.

(20) Valeur, B. *Molecular Fluorescence: Principles and Applications*; Wiley-VCH: Weinheim, 2002.

(21) Dexter, D. L. *J. Chem. Phys.* **1953**, *21*, 836−850.

(22) (a) Harcourt, R. D.; Scholes, G. D.; Speiser, S. *J. Chem. Phys*. **1996**, *105*, 1897−1901. (b) Harcourt, R. D.; Scholes, G. D.; Ghiggino, K. P. *J. Chem. Phys*. **1994**, *101*, 10521−10525.

(23) Turro, N. J. *Modern Molecular Photochemistry*; University Science Books: Sausalito, CA, 1991.

(24) Turro, N. J.; Liu, K.-C.; Show, M.-F.; Lee, P. *Photochem. Photobiol.* **1978**, *27*, 523−529.

(25) Klessinger, J. M.; Michl, J. *Excited States and Photochemistry of Organic Molecules*; VCH: New York, 1995.

(26) Meer, B. W. *Resonance Energy Transfer: Theory and Data*; VCH: New York, 1994.

(27) (a) Barashkov, N. N.; Sakhno, T. V.; Nurmukhanmetov, R. N.; Khakel', O. V. *Russ. Chem. Rev.* **1993**, *62*, 539−552. (b) Brouwer, F. Structure Aspects of Exciplex Formation. In *Conformational Analysis of Molecules in Excited States*; Waluk, J., Ed.; Wiley-VCH: New York, **2000**; pp 177−236, and refs cited therein.

(28) TDDFT calculations were performed at the B3LYP level with a 6-31G** basis set, employing the Gaussian03 suite of programs. Starting with the X-ray geometries, the structures were optimized by energy minimization.

(29) See for example: (a) Cassoux, P. *Science* **2001**, *291*, 263−264. (b) Tanaka, H.; Okano, Y.; Kobayashi, H.; Suzuki, W.; Kobayashi, A. *Science* **2001**, *291*, 285−287. (c) Kobayashi, A.; Tanaka, H.; Kobayashi, H. *J. Mater. Chem.* **2001**, *11*, 2078−2088.

(30) See for example (a) Zheng, S.-L.; Zhang, J.-P.; Wong, W.-T.; Chen, X.-M. *J. Am. Chem. Soc.* **2003**, *125*, 6882−6883. (b) Zheng, S.-L.; Zhang, J.-P.; Chen, X.-M.; Huang, Z.-L.; Lin, Z.-Y.; Wong, W.-T. *Chem. Eur. J.* **2003**, *9*, 3888−3896. (c) Zheng, S.-L.; Chen, X.-M. *Aust. J. Chem.* **2004**, *57*, 703−712.

(31) (a) Wilkinson, F.; Leicester, P. A.; Vieira Ferreira, L. F.; Vieira Freire, M. R. *Photochem. Photobiol.* **1991**, *54*, 599−608. (b) Vieira Ferreira, L. F.; Ferreira Machado, I.; Da Silva, J. P.; Oliveira, A. S. *Photochem. Photobiol. Sci.* **2004**, *3*, 174−181, and references therein.

(32) Vieira Ferreira, L. F.; Vieira Ferreira, M. R.; Da Silva, J. P.; Machado, I. F.; Oliveira A. S.; Prata, J. V. *Photochem. Photobiol. Sci.* **2003**, *2*, 1002−1010, and references therein.

(33) (a) Vala, M.; Hurst, J. *Mol. Phys.* **1981**, *43*, 1219−1234. (b) Connors, R. E.; Christian, W. R. *J. Phys. Chem.* **1982**, *86*, 1524−1528.

(34) (a) Scaiano, J. C. *J. Am. Chem. Soc.* **1980**, *102*, 7747−7753. (b) Barra, M.; Bohne, C.; Scaiano, J. C. *J. Am. Chem. Soc.* **1990**, *112*, 8075−8079. (c) Barra, M.; Bohne, C.; Scaiano, J. C. *Photochem. Photobiol.* **1991**, *54*, 1−5.

(35) Zheng, S.-L.; Coppens, P., unpublished results: CMCR-3CH_3CN-2H_2O: $P2/n$, a (Å) = 7.2855, b (Å) = 19.4095, c (Å) = 25.9748, β (°) = 97.836, V (Å^3) = 3638.7; CECR-CH_3CN-4H_2O: $P2/n$, a (Å) = 13.7836, b (Å) = 7.7986, c (Å) = 18.2581, β (°) = 103.157, V (Å^3) = 1911.1; HECR−H_2O-MeOH: $R\bar{3}$, a (Å) = 15.5571, b (Å) = 15.5571, c (Å) = 21.3445, V (Å^3) = 4473.7.

(36) Zheng, S.-L.; Gembicky, M.; Graber, T.; Chen, Y.-S.; Messerschmidt, M.; Dominiak. P.; Vorontsov, I.; Coppens, P., to be published.

(37) Crosby, G. A.; Hager, G. D.; Hipps, K. W.; Stone, M. L. *Chem. Phys. Lett*. **1974**, *28*, 497−500.

(38) Wrighton, M. S.; Pdungsap, L.; Morse, D. L. *J. Phys. Chem*. **1975**, *79*, 66−71.

(39) Kovalevsky, A. Y.; Gembicky, M.; Novozhilova, I. V.; Coppens, P. *Inorg. Chem*. **2003**, *42*, 8794−8802.

(40) Zheng S.-L.; Coppens, P. unpublished results: Cu(dmp)$_2$-(THPE)$^-$: $P2(1)/n$: a (Å) = 14.8897, b (Å) = 17.5952, c (Å) = 15.0067, β (°) = 95.9449, V (Å^3) = 3910.4; Cu(dmp)$_2$-(2THPE)$^-$ -H_2O: $P2(1)/n$: a (Å) = 11.9170, b (Å) = 20.7778, c (Å) = 22.4447, β (°) = 97.9128, V (Å^3) = 5504.6.

CG050247D